Climate Change and the Lower Coquille Watershed

Darrin Sharp
Oregon Climate Change Research Institute (OCCRI)
November, 2012

OCCRI

Table of Contents

Climate Primer

The earth is kept at a livable temperature by the greenhouse effect. About two-thirds of incoming shortwave solar radiation passes through the atmosphere, while one-third is reflected back into space. The solar radiation that is not reflected back to space warms the earth's surface and to a lesser extent the atmosphere. The warm surface re-radiates some of this heat back into the atmosphere, where it is absorbed and re-emitted by atmospheric greenhouse gases (GHGs). As the concentration of GHGs increases, more heat is re-emitted downward, raising the temperature of the earth. Figure 1 illustrates this effect. Additional GHGs in the atmosphere (especially CO_2) are due in large part to the combustion of fossil fuels.

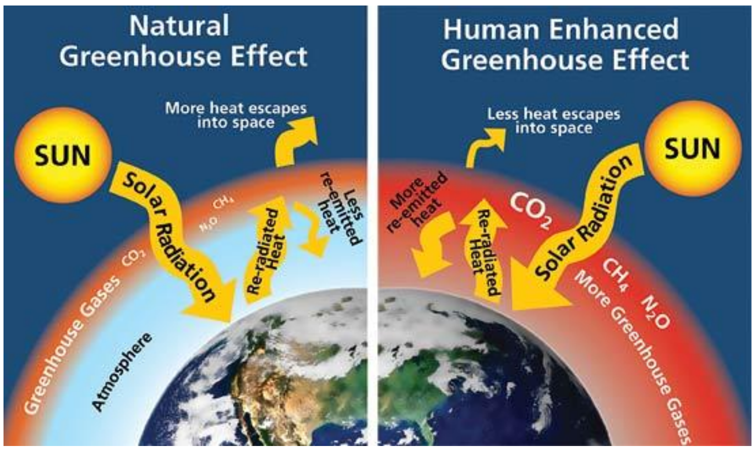

Figure 1: Natural greenhouse effect on the left; enhanced effect on the right.

The concentrations of GHGs, especially CO_2, have been increasing since the Industrial Revolution at the end of the 18th century. Very precise records of the atmospheric concentration of CO_2 have been kept since the late 1950's, as is illustrated in Figure 2. Since pre-industrial times (circa 1750) CO_2 concentrations have risen from approximately 280 ppm to over 390 ppm (IPCC Summary for Policymakers, WG I 2007; NOAA ESRL).

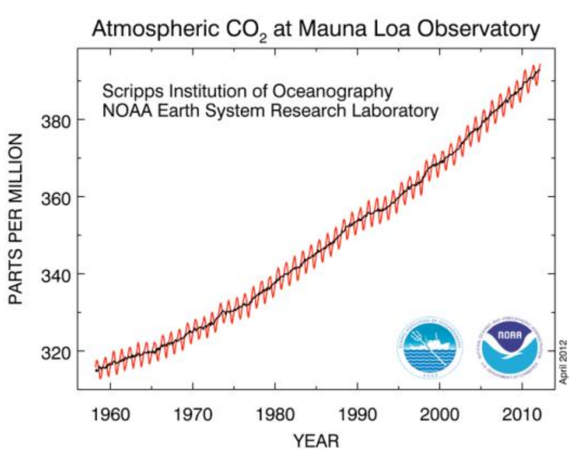

Figure 2: Atmospheric CO_2 concentration measured at the Mauna Loa Observatory in Hawaii.

Uncertainty

There are three primary sources of uncertainty that apply to climate change projections: future GHG emissions; natural climate variability; and the climate sensitivity (Hawkins and Sutton 2009). Each is discussed in turn below.

Future Emissions: Due to unknown technological, social, and political factors that may come into play in the coming years, it is difficult to project future anthropogenic GHG emissions. Societal action (or inaction) could substantially affect the amount of GHGs added to the atmosphere. As a result, climate researchers have developed a suite of possible future emissions outcomes. For the Intergovernmental Panel on Climate Change (IPCC) Fourth Assessment Report (AR4) a number of emissions scenarios (storylines) were developed that each encompassed a set of socioeconomic, political, demographic and technological assumptions (IPCC Summary for Policymakers, WG I 2007). Figure 3 illustrates projected CO_2 emissions for several scenarios used in AR4. For the IPCC Fifth Assessment Report (AR5, due in 2013) a new framework for representing possible future emissions was developed. For AR5, four radiative forcing trajectories, known as Representative Concentration Pathways (RCPs), are defined. Each RCP corresponds to a certain radiative forcing applied to the climate system (where a higher radiative forcing corresponds to a higher concentration of GHGs, and a greater degree of warming). Four RCPs are defined in order to eliminate the notion that a middle pathway is the most likely. See Figure 4. The label of each RCP (2.6, 4.5, 6.0, 8.5) indicates how much additional forcing (in watts/m^2) it would produce in 2100.

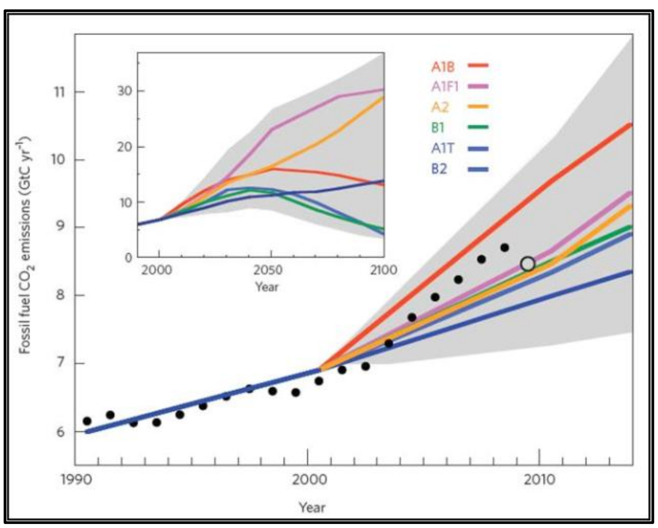

Figure 3: IPCC AR4 emissions scenarios. Black dots are actual emissions (Manning et al. 2010).

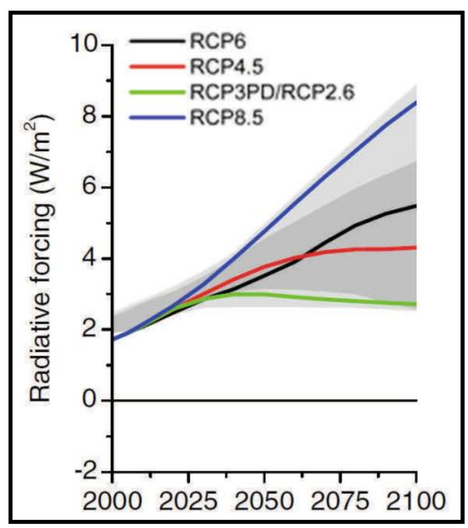

Figure 4: Representative Concentration Pathways (RCPs) (van Vuuren et al. 2011).

Natural Variability: Many factors affect the climate and contribute to its natural variability. This variability is an important component of the uncertainty in climate projections. For example, Figure 5 illustrates the variability in annual mean temperature, which is inherent in the climate from year-to-year. On short time scales, the natural variability in the climate can mask (or accentuate) long-term climate trends.

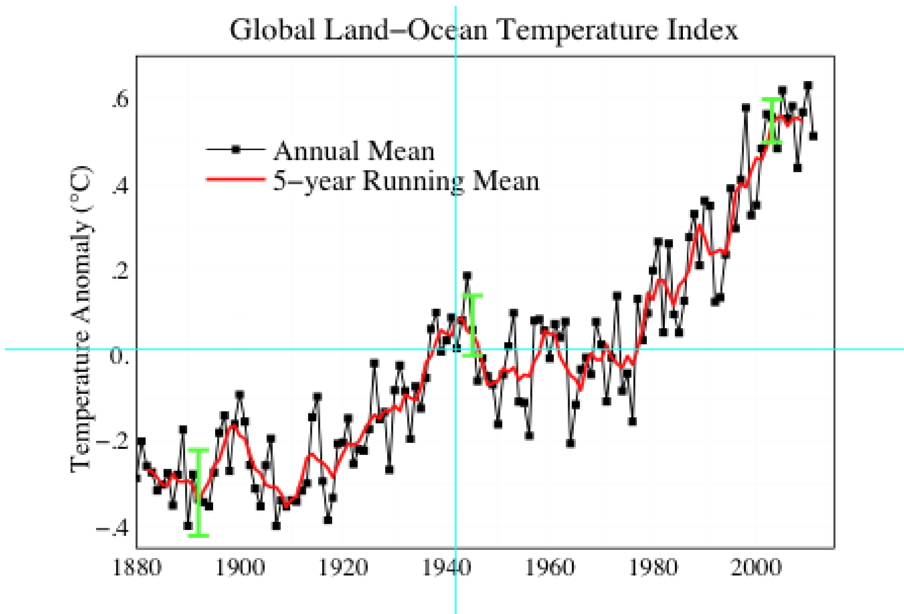

Figure 5: Global land-ocean temperature index. Green bars are the 2-sigma error estimates (95% CI) (NASA GISS; Hansen et al. 2010).

Climate Sensitivity: The response of the climate system to an increase of GHGs is the third source of uncertainty in climate projections. The uncertainty of this response stems from uncertainties in the underlying processes (for example, cloud physics). The climate sensitivity (defined here as the change in the global temperature due to a doubling of the atmospheric concentration of CO_2) is a convenient measure of the climate's response to GHGs. Figure 6 illustrates the probability distributions of several published climate sensitivities. As the figure shows, the most likely climate sensitivity is in the range of 2.5-3.5°C/4.5-6.3°F. But, a climate sensitivity lower, or substantially higher, than that cannot be ruled out.

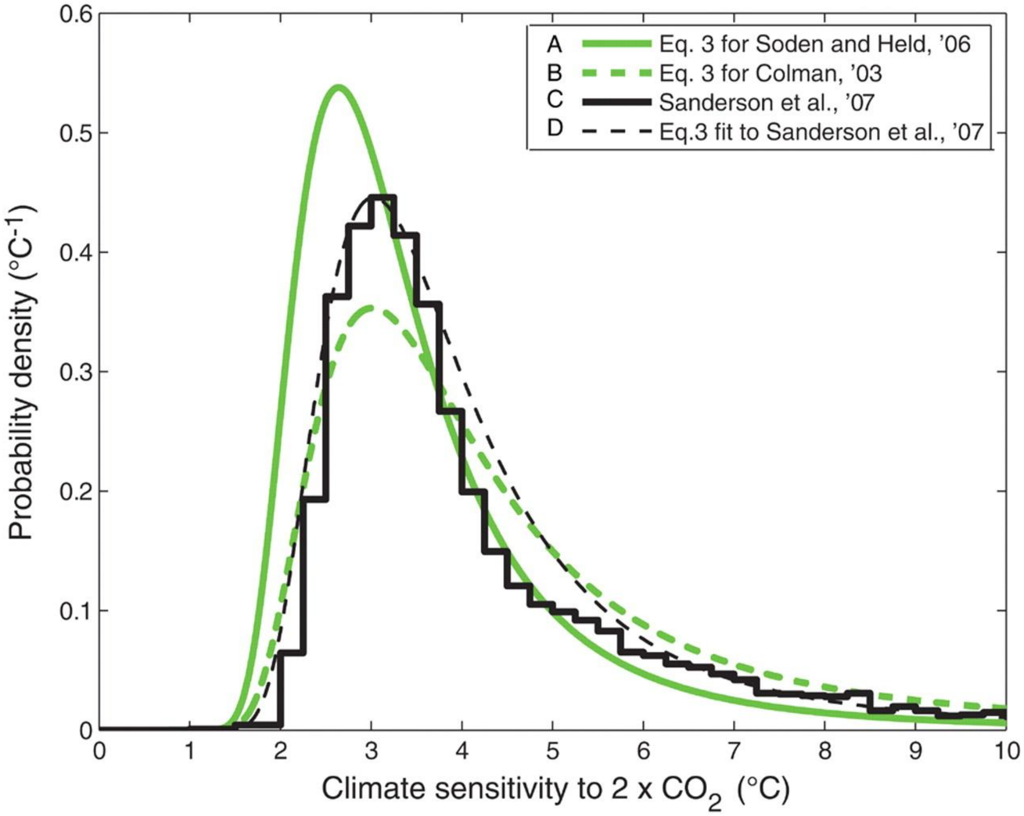

Figure 6: Probability distribution of climate sensitivity (Roe and Baker 2007).

The above three sources of uncertainty are summarized in Figure 7. This figure illustrates the relative contribution to overall uncertainty of mean decadal temperature from each of the three sources. The left panel of the figure illustrates uncertainty from a global perspective, while the right panel illustrates uncertainty from a regional perspective.

Note that as the lead time increases (i.e. the number of years into the future), it is the uncertainty in GHG concentrations that dominates. With shorter lead times, the climate sensitivity of the models is a larger source of uncertainty. For regional projections, natural climate variability can dominate into the first couple of decades. The implication of this is that projecting the effect of increased GHGs on a regional (and even more so, local) level is much more difficult than projecting the effect at the global level.

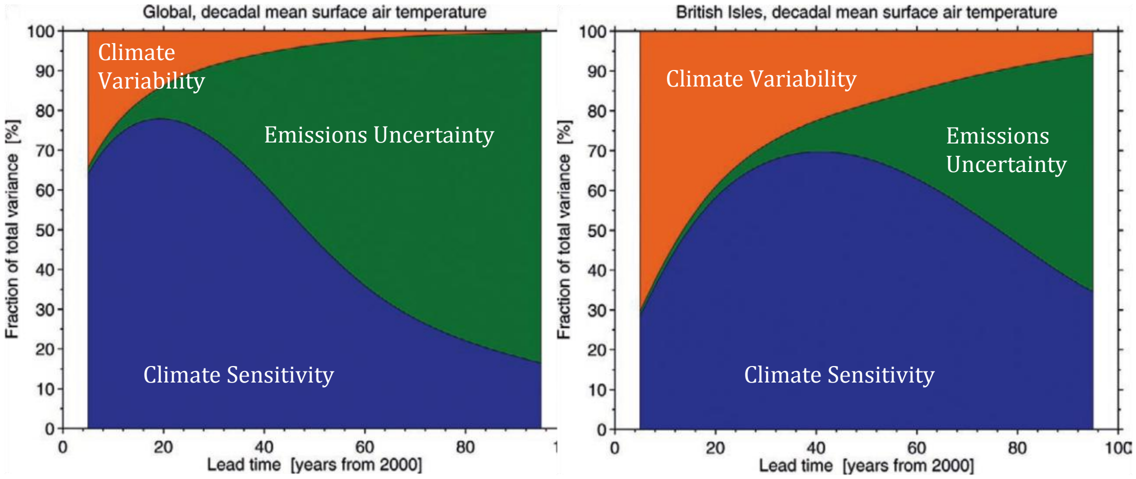

Figure 7: A comparison of the relative contribution of the three sources of uncertainty as they change with the lead time of the projection, and as they differ from global to regional projections. Green = emissions uncertainty; Orange = climate variability; Blue = climate sensitivity (Hawkins and Sutton 2009).

As noted above, any attempt at projecting future climate entails incorporating a number of underlying uncertainties and assumptions into the projection. Using ensembles (or suites) of models is one way of addressing the uncertainty in projections. The mean, median, percentiles, and spread/range of an ensemble of model projections can give insight into possible realizations of future climate. Given all the possible input permutations (emissions scenarios, model sensitivities, etc.), even an ensemble of models may not represent all possible future realizations of climate. Even so, the projections produced by model ensembles can be useful tools for investigating the impacts of climate change.

To that end, wherever possible, projections in this report are based on multi-model ensembles and checked for consistency with other projections based on similar assumptions. The assumptions made, for example the emissions scenario chosen, are ones that could reasonably be expected to occur in the future (i.e. no "extreme" assumptions were made in order to investigate the edges of the projection envelope).

Ultimately, the application of climate projections to management decisions will depend on the time frame of interest and the level of risk tolerance.

Historical Data/Future Projections

Temperature and Precipitation

Figures 8 and 9 illustrate the results from a recent analysis of temperature and precipitation trends near the Coquille estuary from 1903-2010. Mean monthly temperature and total monthly precipitation from the United States Historical Climatology Network station in North Bend, Oregon (#356073) were analyzed (USHCN). North Bend is the closest station in this data set to the Coquille estuary. Figure 8 (Mean temperature) shows a statistically significant increase in temperature over the analysis period. There has been a warming trend of 0.1 °C/0.2°F per decade. While this trend has varied by season, all seasons show a warming trend. Figure 9, however, shows that there is no statistically significant trend in precipitation over this period.

Research is currently in progress within OCCRI using the Regional Climate Prediction Dot Net (RegCPDN) framework to evaluate both historical and future extreme precipitation events for a domain that includes the Coquille estuary.

Figures 10-13 illustrate the results of an analysis done by the Oregon Climate Change Research Institute regarding future temperature and precipitation trends. Figure 10 illustrates the location of the points used for the analysis; Figures 11-13 are the results. The analysis used projections from a suite of nine regional climate models; six models from the North American Regional Climate Change Assessment Program (NARCCAP) at the University Center for Atmospheric Research (UCAR – www.narccap.ucar.edu),and three models from the USGS Regional Climate Modeling effort at Oregon State University (www.regclim.coas.oregonstate.edu). All projections use the A2 emissions scenario, which is in the middle of the range of scenarios used in the AR4 (see Figure 3 for A2 emissions). All projected changes are relative to averages from the baseline period of 1971-1999.

These figures indicate higher temperatures in the mid-21st century, with the summer months showing the greatest increase. The change in mid-century precipitation is not as clear, but the data suggests the summer months will be somewhat drier.

Figure 11 illustrates the modeling results for a point nearly on the coast, slightly north of the estuary (43.2N, 124.4W). Figure 12 is the result for 43.2N, 124.2W (just north of the Coquille), and Figure 13 is for 43.2N and 124.0W (i.e. on the western border of the Coast Range). These three points are shown so the effect of an increase in the distance from the coast can be assessed.

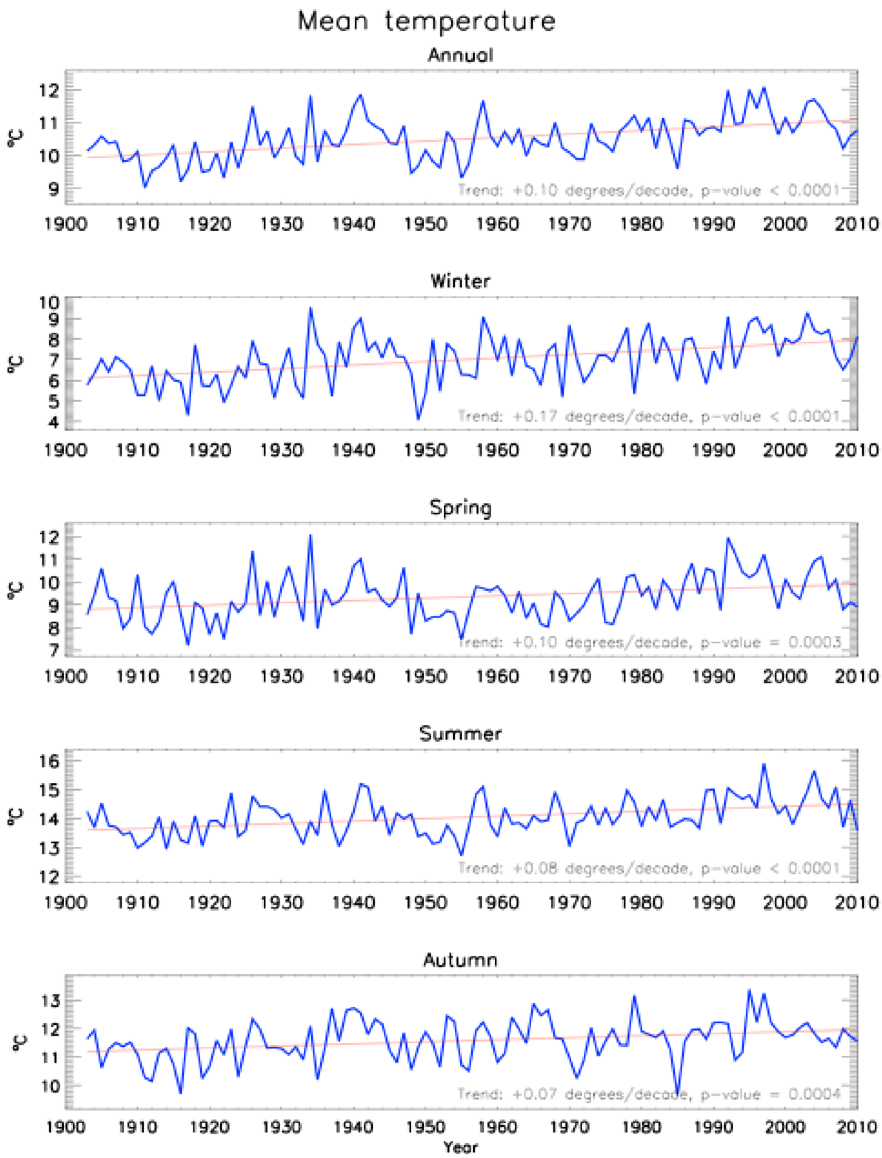

Figure 8: Mean temperature from the Historical Climate Network station in North Bend, OR.

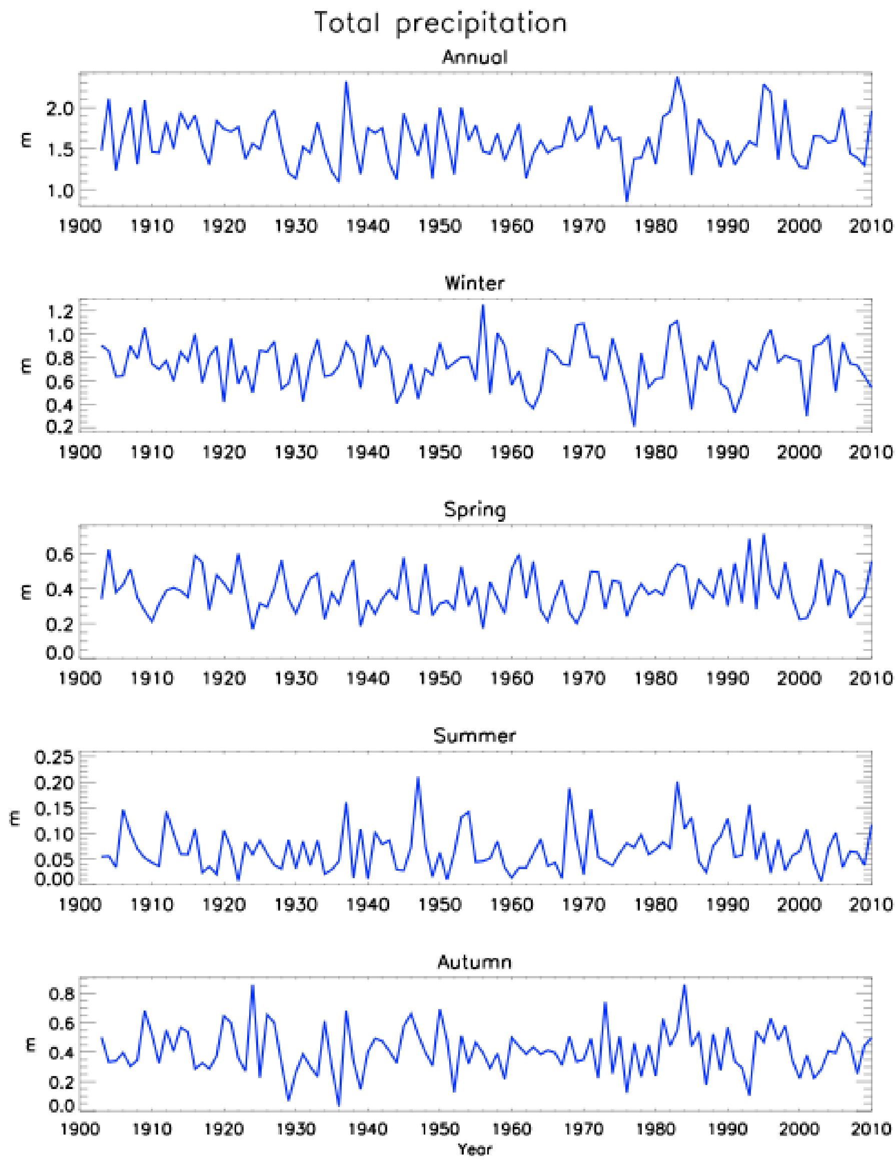

Figure 9: Total precipitation from the Historical Climate Network station in North Bend, OR.

Figure 10: Location of modeling points

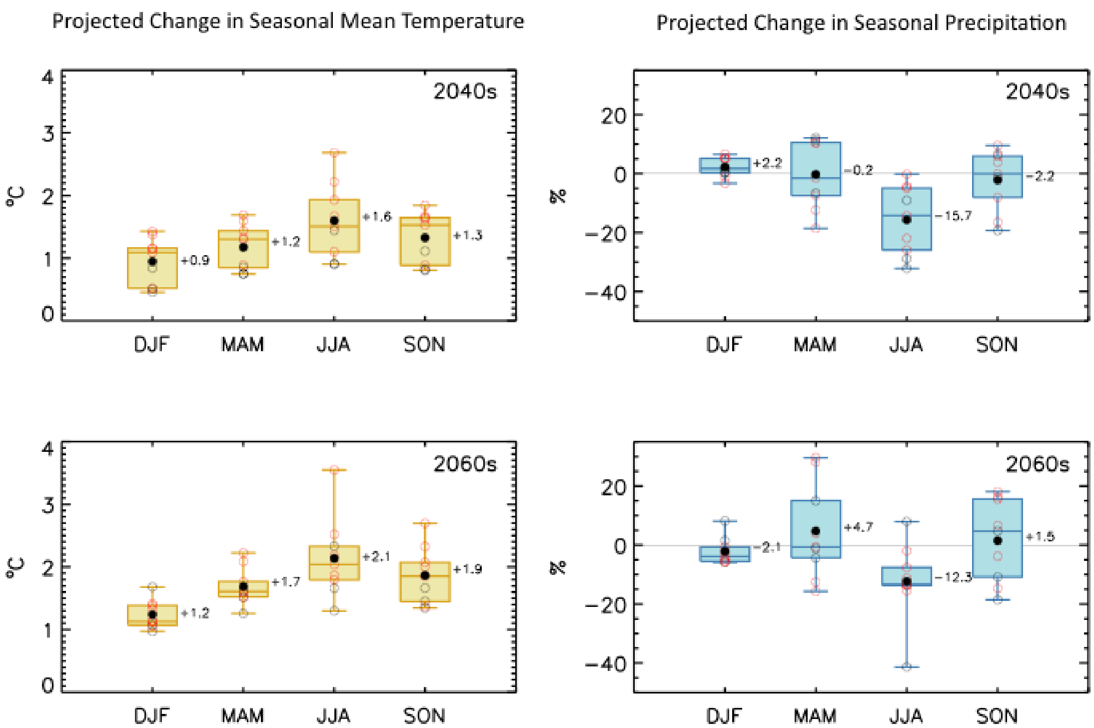

Figure 11: Projected change in seasonal mean temperatures and projected percent change in seasonal precipitation in the 2040s and 2060s for 43.2N, 124.4W. Projections are derived from six NARCCAP simulations (red circles) and three RegCLIM simulations (black circles). Solid black dot is the mean; the box represents the 25th, 50th, and 75th percentiles for the nine simulations evaluated, with the top of the box being the 75th percentile, the middle line being the 50th percentile (median), and the bottom of the box being the 25th percentile; error bars indicate the extremes. DJF = DecJanFeb (Winter), MAM = MarAprMay (Spring), JJA = JunJulAug (Summer), SON = SepOctNov (Fall).

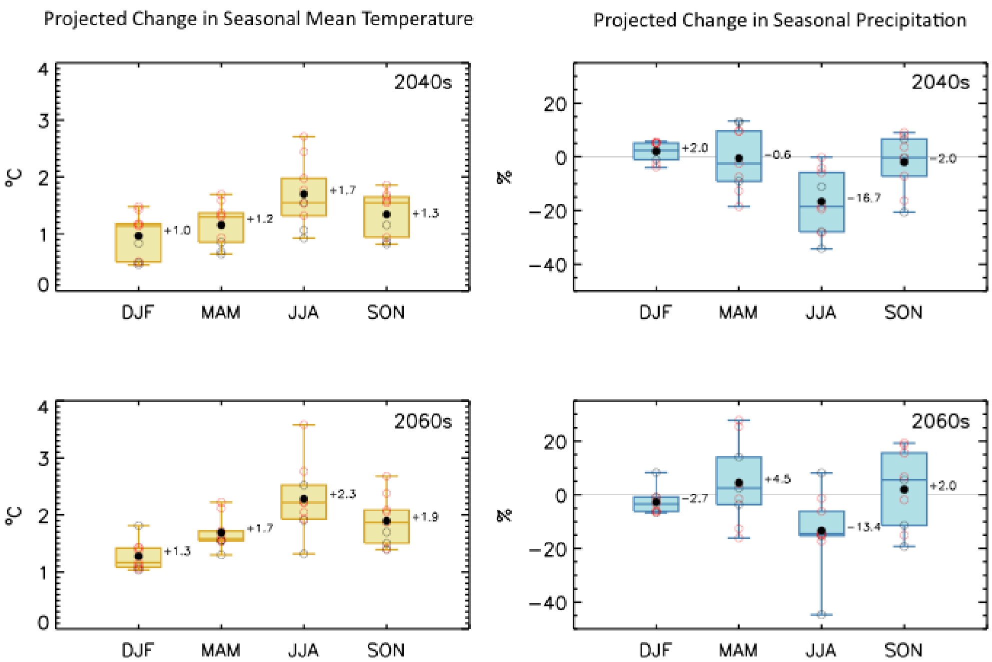

Figure 12: As above, except for 43.2N, 124.2W.

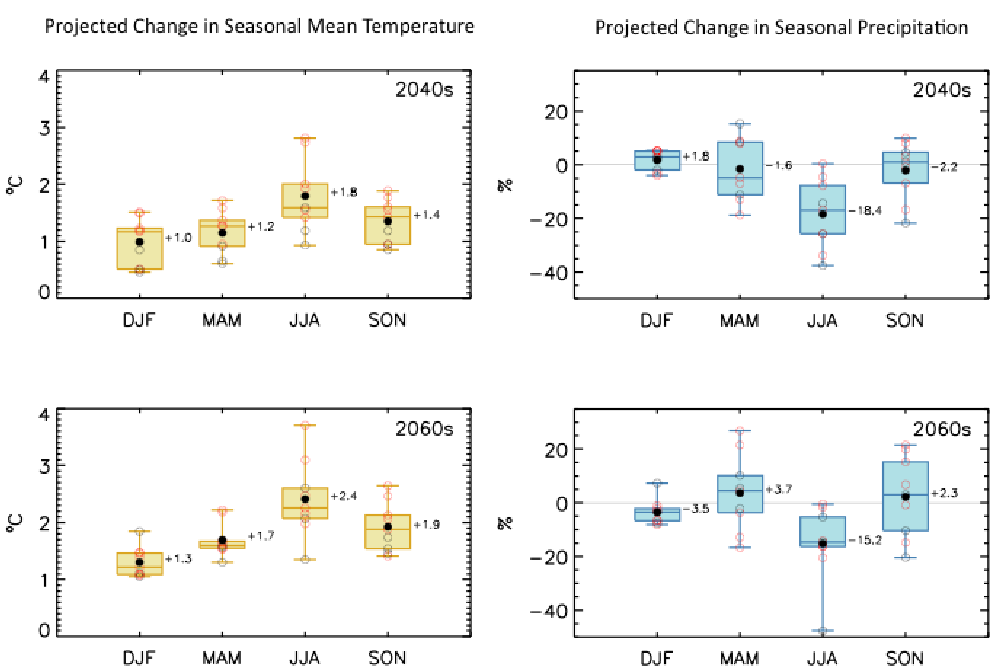

Figure 13: As above, except for 43.2N, 124.0W.

For comparison, Figures 14 and 15 show the results of a similar analysis done by the University of Washington (UW) Climate Impacts Group (CIG) for the entire Coquille Basin (Hydrologic Unit Code 17100305). While the two sets of results cannot be compared directly due to the use of different emissions scenarios, different time frames, and different climate models, it is useful to compare the broad trends. In general terms, the two projection efforts show similar results. Namely:

- All model simulations project increased temperatures by mid-century, with the greatest increases during the summer months.

- There is less certainty in precipitation trends. The range of simulations encompasses both an increase and a decrease in annual precipitation by mid-century.

Other recent efforts have attempted to quantify potential changes in extreme precipitation events in addition to changes in annual or seasonal means. When considering ensemble averages (i.e. the averages produced by an ensemble of climate models), Dominguez et al. (2012) found minimal changes to projected mean winter precipitation levels for the area encompassing the Coquille estuary in the mid-21st century. However, they did find a statistically significant increase in 20 and 50 year return period winter one-day precipitation totals for this domain.

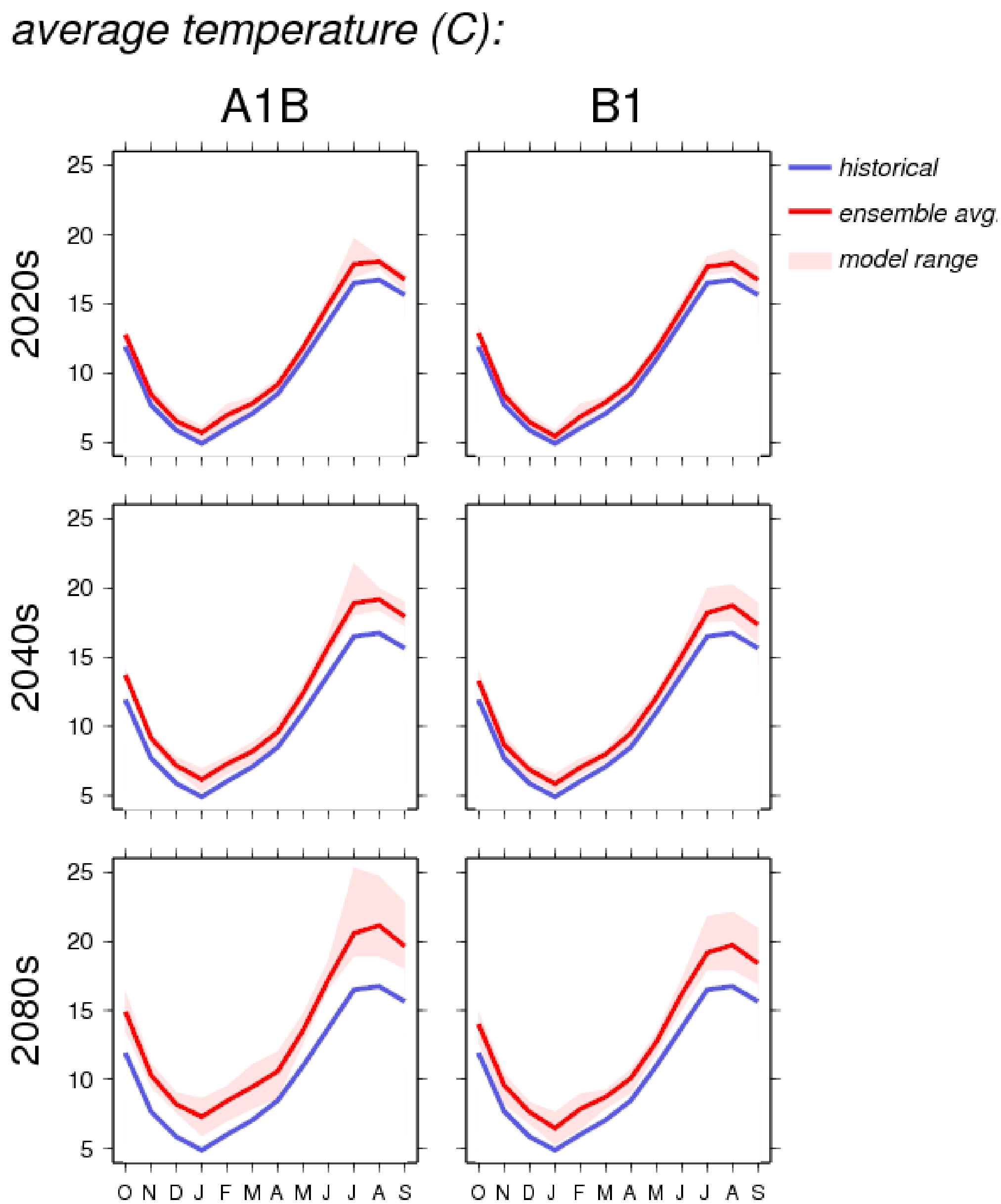

Figure 14: UW CIG monthly average temperature projections. A1B and B1 emissions scenarios. O = Oct, N= Nov, etc. (Mauger and Mantua 2011).

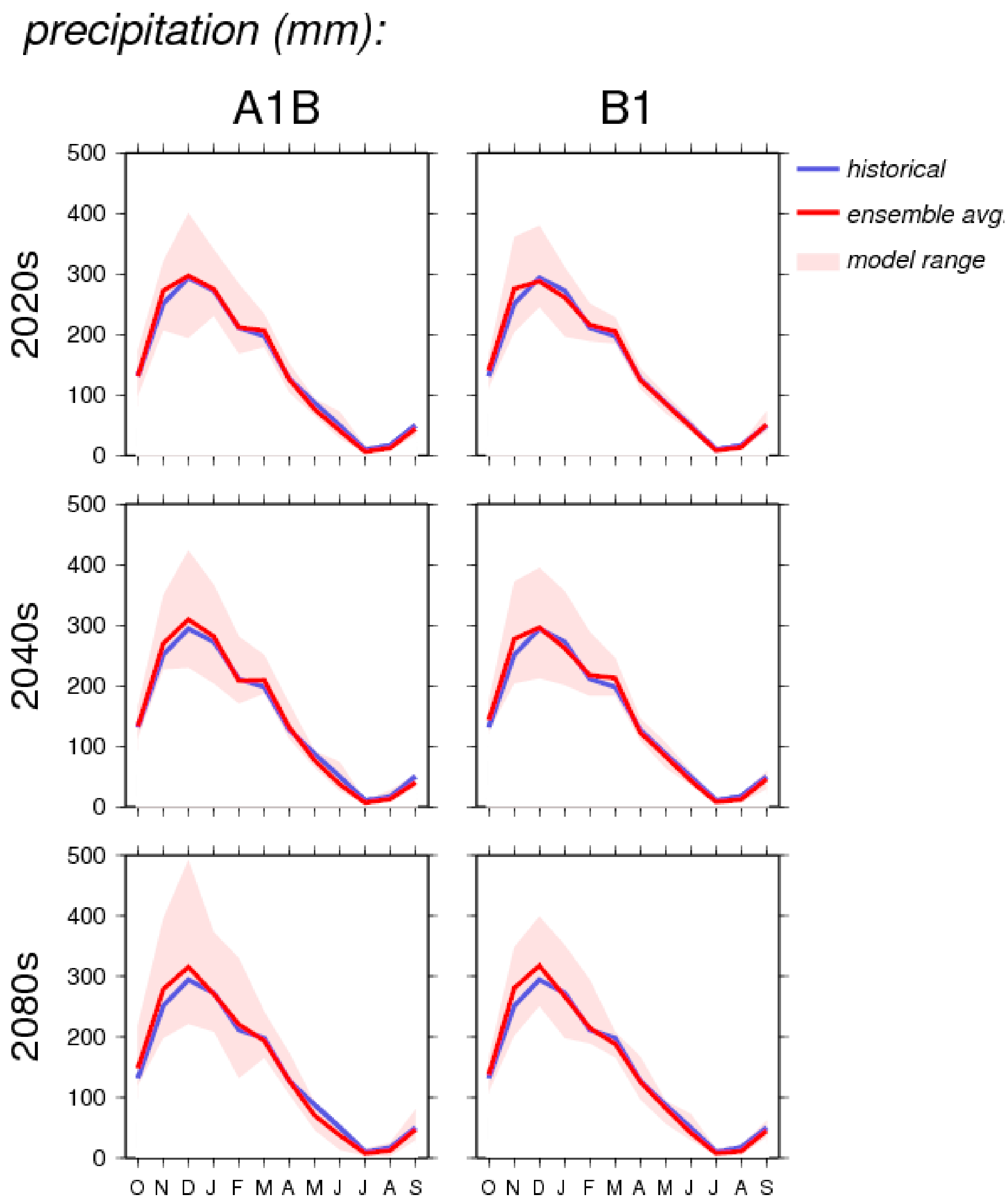

Figure 15: UW CIG monthly total precipitation projections. A1B and B1 emissions scenarios. O = Oct, N= Nov, etc. (Mauger and Mantua 2011).

Ocean Acidification

In addition to the projected climate impacts of increased atmospheric GHGs, an increasing atmospheric CO_2 concentration has changed and will continue to change the chemistry of ocean waters, making them more acidic. This increase in acidity (i.e. a lower pH) is known as ocean acidification. Changes in ocean pH may have important biological effects. Marine organisms known as calcifiers rely on the process of calcification to build and maintain their hard body parts. Such organisms include shellfish, corals, and some plankton.

In the simplest terms, the chemical equation that controls the calcification rate is shown below:

$$CO_3^{2-} + Ca^{2+} \Leftrightarrow CaCO_3$$

In a more acidic environment, carbonate ions (CO_3^{2-}) are not as plentiful and the equation above moves to the left (away from $CaCO_3$, a key component of hard body parts). This leftward movement implies that calcifiers may have difficulty building or maintaining their hard body parts.

The overall chemistry involved in this process is shown in Figure 16 below. Longer arrows indicate reactions that are enhanced by an increase in the atmospheric CO_2 concentration. Note that as ocean acidity increases (denoted by an increase in H^+ ions), H^+ ions combine with CO_3^{2-} (carbonate ions) to produce bicarbonate ions. As a result, fewer carbonate ions are available to calcifiers.

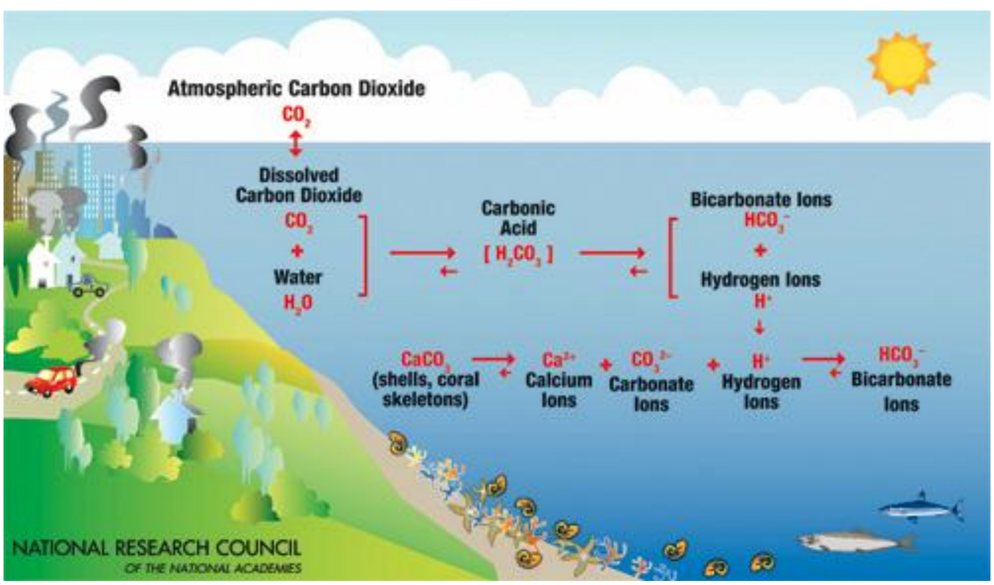

Figure 16: Ocean chemistry, illustrating the effect of increased atmospheric CO^2.

The ultimate effect of ocean acidification on calcifiers is still an active research topic. Ocean acidification is an important consideration for the Coquille estuary, due to past and projected increases in acidification along the entire Oregon coast. For example, by 2050 the nearshore 10 km domain may see an annual mean pH as low as 7.82 ± 0.04 (compared to a pre-industrial value of 8.03 ± 0.03) (Gruber et al. 2012).

Over the past 250 years, since the beginning of the industrial revolution, there has been about a 16% decrease in aragonite and calcite saturation state in the Pacific Ocean due ocean acidification processes (Feely et al., 2012). (The saturation of calcium carbonate is observed in its two most common polymorphs, aragonite and calcite.) Feely and colleagues recently published the results of repeat oceanographic surveys in the Pacific Ocean showing accelerating ocean acidification trends over the past 14-year period. The observations show an average 0.34% per year decrease in the aragonite and calcite saturation state of surface seawater. This has caused an upward migration of the aragonite and calcite saturation horizons toward the ocean surface on the order of 1–2 m per year. (Calcifying organisms live above the aragonite and calcite saturation horizon.)

Virtually every major biological function of marine organisms has been shown to respond to acidification changes in seawater, including photosynthesis, respiration rate, growth rates, calcification rates, reproduction, and recruitment. Much of the attention has focused on carbonate-based animals and plants which form the foundation of our marine ecosystems. An increase in ocean acidity has been shown to impact shell-forming marine organisms from plankton to benthic molluscs, echinoderms, and corals (Doney et al. 2009; Barton et al. 2012). Many calcifying species exhibit reduced calcification and growth rates in laboratory experiments under high-CO_2 conditions. For example, in the Netarts estuary in Oregon, it was demonstrated that increased acidification negatively impacted oyster production, due to decreased vigor in later life stages (Barton et al. 2012). Ocean acidification also causes an increase in carbon fixation rates in some photosynthetic organisms (both calcifying and noncalcifying). (Feely et al. 2012; Doney et al. 2009; Smith and Baker 2008; and Ocean Carbon and Biogeochemistry Program 2008).

Sea Level Rise

Two primary factors contribute to global sea level rise: thermal expansion of the oceans as their temperatures rise due to greenhouse warming; and an increase in water volume as land ice melts and the water makes its way into the oceans (NRC 2012). Previously, it was thought that thermal expansion was the primary contributor to global sea level rise (Bindoff et al. 2007). Recent research shows that the melting of ice is now the primary contributor (~65%) to the recent (1993-2008) rise in sea levels worldwide (NRC 2012).

Figure 17 illustrates global sea level rise since 1870, estimated using a combination of tide gauge and satellite data.

Sea Level Rise Data from NASA, http://climate.nasa.gov/keyIndicators/#seaLevel

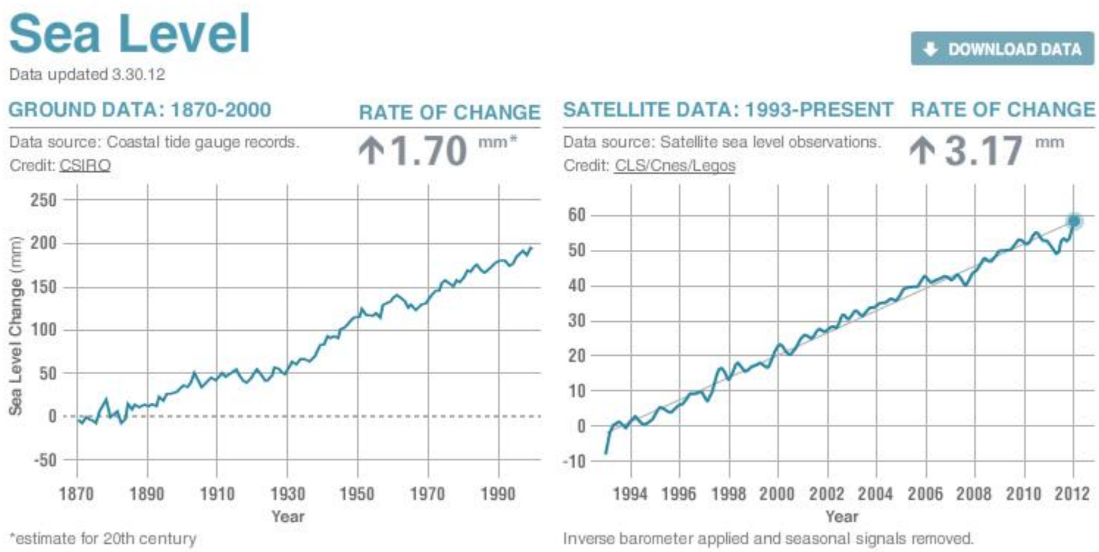

Figure 17: Global sea level rise.

Global (and regional) sea level rise projections have been calculated by various groups and authors. A recent National Research Council (NRC) report on sea level rise along the west coast generated its own set of projections and compared them to two other well known sea level rise projection efforts. Figure 18 summarizes the findings. Vermeer and Rahmstorf (2009) is a semi-empirical method based on the observed historical correlation between global temperature and sea level change; IPCC (2007) is the model-based projection from the IPCC's Fourth Assessment Report (Working Group I). These two sets of projections were chosen for comparison as they are representative of semi-empirical and model-based sea level rise projection methodologies (respectively).

While the NRC (2012) projection values for sea level rise in 2030 and 2050 are similar to Vermeer and Rahmstorf, they have a somewhat wider range. For 2100, the NRC committee projects a rise which is substantially higher than the IPCC (2007), but at the lower end of the Vermeer and Rahmstorf range. Table 1 summarizes the NRC 2012 global projections in tabular form.

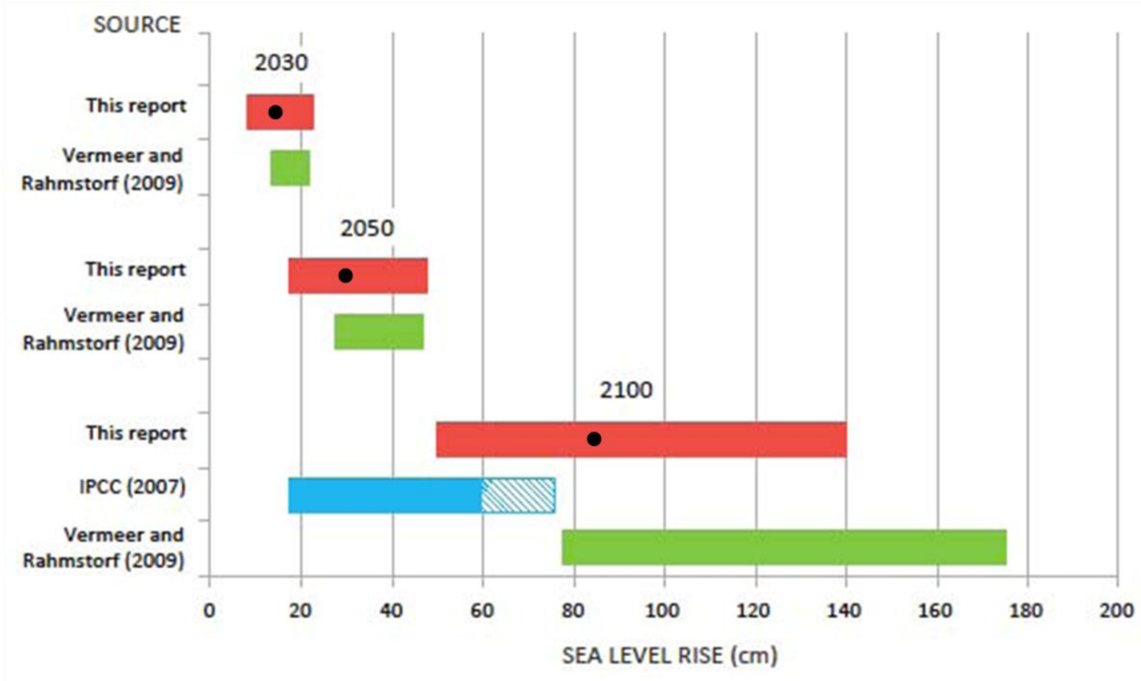

Figure 18: Global sea level rise projections for 2030, 2050, and 2100. Dots are the projection, bars are the range. For IPCC, diagonal lines are for scaled-up ice sheet discharge (NRC 2012). The bars labeled "This report" refer to NRC 2012.

Global Sea-Level Rise Projections (cm) Relative to Year 2000					
2030		2050		2100	
Projection	Range	Projection	Range	Projection	Range
13.5±1.8	8.3-23.2	28.0±3.2	17.6-48.2	82.7±10.6	50.4-140.2

Table 1: NRC 2012 global sea level rise projections.

Sea levels along the US west coast are impacted by global sea level rise, as well as regional effects such as: ocean and atmospheric circulation patterns (e.g. the El Niño-Southern Oscillation (ENSO), and the Pacific Decadal Oscillation (PDO)); the effects of land ice mass changes; groundwater withdrawal or recharge; and tectonics along the coast. Along the west coast the relative sea level is raised by the warm phase of ENSO (El Niño) and the PDO, and negative vertical land motion (i.e. subsidence). Conversely, the cool phase of the ENSO (La Niña) and the PDO, as well as positive vertical land motion (i.e. uplift/emergence) lowers relative sea level. A strong El Niño can elevate sea level along the west coast by 10-30 cm for several months in the winter (NRC 2012).

Vertical land motion along the west coast is driven by a variety of geological factors. The net result is that the coast north of Cape Mendocino, CA is rising (i.e. positive vertical land motion), and the coast south of Cape Mendocino is falling (NRC 2012). The rate of vertical land motion, however, can vary even within this broad characterization (Komar et al. 2011). Specifically, these findings show that the southern Oregon coast and the Coquille Estuary area have vertical land movements that to date, completely offset the effects of global sea level rise with approximately 0.5 to 1.2 mm/yr.net sea level *decrease*.

Table 2 presents projections for local sea level rise along the west coast. These projections include all the factors mentioned above (thermal expansion, melting ice, vertical land motion, etc.). Note how projections for areas north of Cape Mendocino (Seattle and Newport) are lower than for those south of that point (due primarily due to the difference in vertical land motion). Figure 19 summarizes graphically the findings of NRC 2012 for regional and global sea level rise as compared to the semi-empirical approach.

Regional Sea-Level Rise Projections (cm) Relative to Year 2000						
	2030		**2050**		**2100**	
Location	**Projection**	**Range**	**Projection**	**Range**	**Projection**	**Range**
Seattle	6.6 ± 5.6	-3.7-22.5	16.6 ± 10.5	-2.5-47.8	61.8 ± 29.3	10.0-143.0
Newport	6.8 ±5.6	-3.5-22.7	17.2 ± 10.3	-2.1-48.1	63.3 ± 28.3	11.7-142.4
San Francisco	14.4 ± 5.0	4.3-29.7	28.0 ± 9.2	12.3-60.8	91.9 ± 25.5	42.4-166.4
Los Angeles	14.7 ± 5.0	4.6-30.0	28.4 ± 9.0	12.7-60.8	93.1 ± 24.9	44.2-166.5

Projection = mean ± std deviation for A1B emissions
Range = means for B1 (low) and A1FI (high) emissions

Table 2: West coast sea level rise projections (NRC 2012).

NRC 2012 uses a necessarily conservative approach to vertical land movement due to a lack of sufficient data points for the entire west coast and the complicating issue of local sediment compaction and/or fluid withdrawal. However, it is important to consider analyses that do incorporate more data, such as Komar et al. 2011, and Telbaldi et al. 2012. These additional analyses provide sea level projections for the six tide gauges located in Oregon and Washington, including the gauge at Coos Bay, using the semi-empirical approach of Vermeer and Rahmstorf (2009) with vertical land motion and other local factors taken into account using historical data from each gauge station. While a single data point (such as Coos Bay) should not be generalized, that data point does support trends found by Komar et al. (2011) which show less impact from sea level rise along the southern coast of Oregon. Table 3 illustrates expected relative sea level rise values from an ensemble mean of models. The values listed are the rise above 2008 levels by 2030 and 2050 in meters/inches.

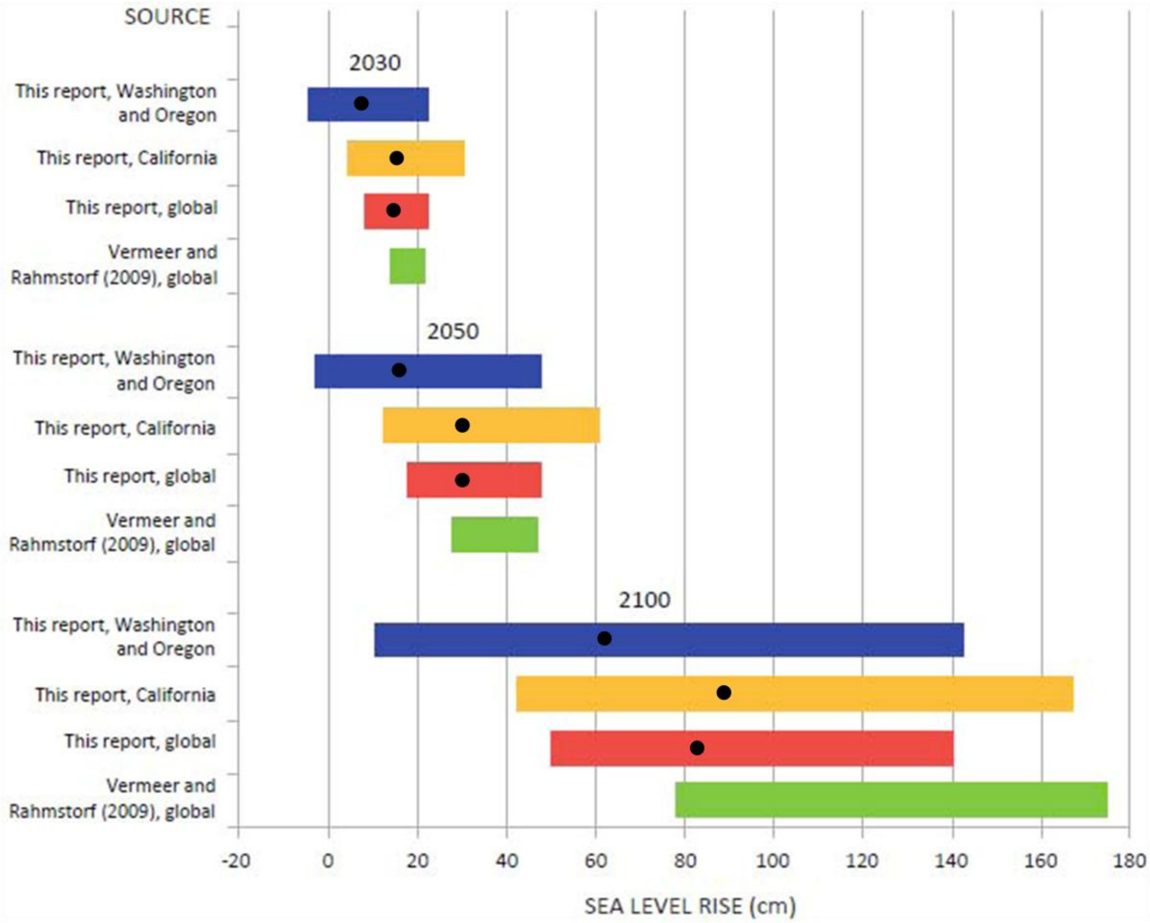

Figure 19: Global and regional sea level rise. Dots are the projection, bars indicate the range (NRC 2012). The bars labeled "This report" refer to NRC 2012.

	Sea Level Rise (m/in)	
Station	**2008-2030**	**2008-2050**
Charleston, Coos Bay, OR	0.09/3.5"	0.24/9.4"
South beach, Yaquina R., OR	0.12/4.7"	0.30/11.8"
Astoria, Tongue Pt., Col. R., OR	0.07/2.8"	0.19/7.5"
Toke Pt., Willapa Bay, WA	0.10/3.9"	0.25/9.8"
Neah Bay, Strait of Juan de Fuca, WA	0.03/1.2"	0.11/4.3"
Seattle, Puget Sound, WA	0.11/4.3"	0.28/11.0"

Table 3: Expected sea level rise based on an ensemble mean of models of relative sea level rise. Quantities indicate the amount of relative sea level rise from 2008 to 2030 and 2008 to 2050 in meters/inches (Tebaldi et al., 2012).

Tebaldi et al. (2012) show that these seemingly low increases in sea level will have significant impacts in the short term when storm surges are taken into account (Tables 4 and 5). Historic data are used to estimate future return periods for what today are considered 50-year and 100-year events. This magnifies sea level rise by a factor of five, on average, as shown below and dramatically increases the occurrence, or return periods, of storm surge events.

	Return Level (m/in)	
Station	**50 year**	**100 year**
Charleston, Coos Bay, OR	1.29/50.8”	1.33/52.4”
South beach, Yaquina R., OR	1.31/51.6”	1.37/53.9”
Astoria, Tongue Pt., Col. R., OR	1.34/52.8”	1.36/53.5”
Toke Pt., Willapa Bay, WA	1.85/72.8”	1.96/77.2”
Neah Bay, Strait of Juan de Fuca, WA	1.44/56.7”	1.47/57.9”
Seattle, Puget Sound, WA	1.20/47.2”	1.23/48.4”

Table 4: Projected 50-and 100-year return levels of storms in meters/inches above mean high water, where mean high water is computed according to gauge epoch, generally 1983-2001 (Tebaldi et al. 2012).

Station	Return Period for 100-yr Floods in 2050
Charleston, Coos Bay, OR	Will occur every 5 years
South beach, Yaquina R., OR	Will occur every 5 years
Astoria, Tongue Pt., Col. R., OR	Will occur every 5 years
Toke Pt., Willapa Bay, WA	Will occur every 30 years
Neah Bay, Strait of Juan de Fuca, WA	Will occur every 20 years
Seattle, Puget Sound, WA	Will occur every 2 years

Table 5: Projected return periods, by 2050, for floods currently qualifying as 100-year events for the ensemble average estimate of relative sea level rise at each gauge (Tebaldi et al. 2012).

Hydrology/Stream Flow

As is typical of many of the rivers in the Pacific Northwest,the Coquille exhibits a high degree of seasonality in stream flow (Figure 20). Temperature and precipitation modeling results suggest that climate change may emphasize this pattern; higher summer temperatures and decreased precipitation may increase evapotranspiration and decrease summer stream flows (OCAR 2010).

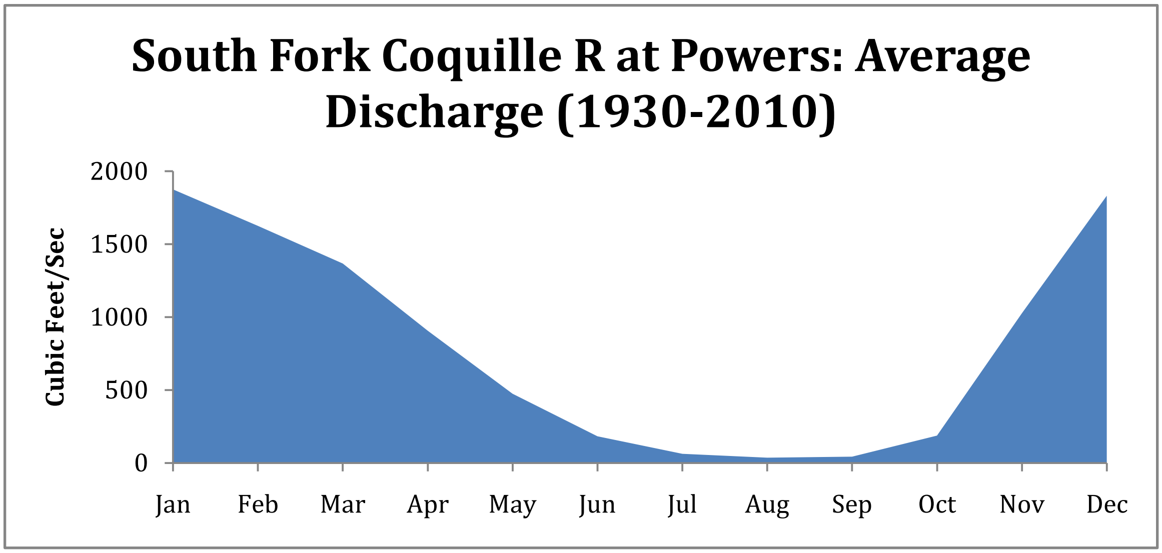

Figure 20: Coquille River average discharge.

Figure 21 illustrates the January and August discharge for the Coquille River at Powers, with trend lines. Note the much higher discharge in January as compared to August.

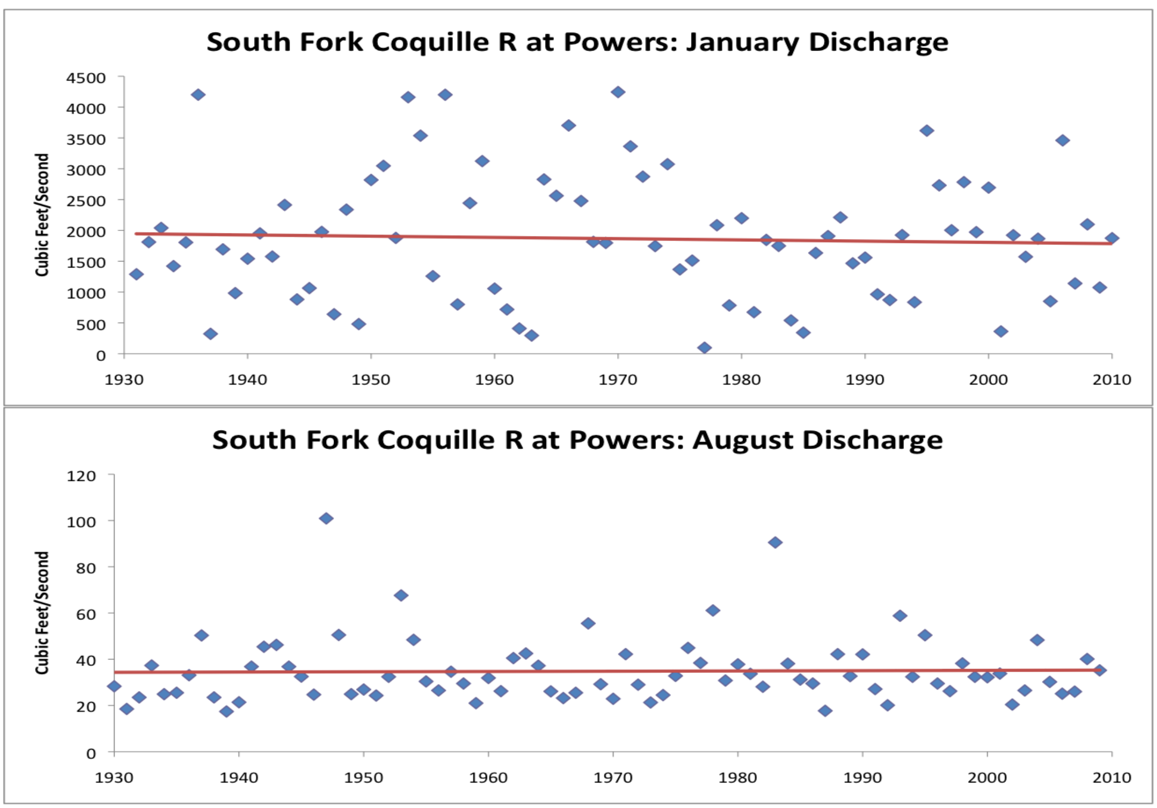

Figure 21: South Fork Coquille River Jan/Aug discharge, 1930-2010. Note the considerable difference in the Y axis.

Another factor for the watershed hydrology is the possibility of increased extreme events. Evidence is beginnig to emerge at the global scale, that for some types of events, notably heatwaves and precipitation extremes, increases in events are linked to climate change (Coumou and Rahmstorf 2012). Regionally, increases in the intensity of future extreme winter precipitation are projected for the western United States by Dominguez et al. (2012). These researchers project an area-averaged 12.6% increase in 20-year return period (or “20-year rainfall events”) and 14.4% increase in 50-year return period daily precipitation (or “50-year rainfall events”) -- a return period is an estimate of how long it will be between rainfall events of a given magnitude.

Near-coast regions such as the Coquille area are vulnerable to such extreme events known as atmospheric rivers or more commonly as “pineapple express” events. These are long and narrow bands of water vapor brought to the west coast from the south Pacific’s extratropical cyclones or the “warm conveyor belt.” They are characterized by high water vapor content falling as large amounts of precipitation as the west coast’s mountain ranges are encountered. Extreme precipitation, devastating floods, and debris flows occur, especially when heavy rain occurs on preexisting snowpack. (Neiman et al. 2008). Such flood and debris events could become more common and/or more severe in intensity or duration.

Upwelling

Upwelling is an important, fundamentally wind-driven, process off the coast of Oregon. Upwelling brings cold, dense, more acidic, nutrient rich, oxygen poor deep water to the surface. Upwelling can greatly enhance primary productivity, and ultimately the productivity of fisheries. Figure 22 illustrates the seasonality of upwelling off the coast of Oregon.

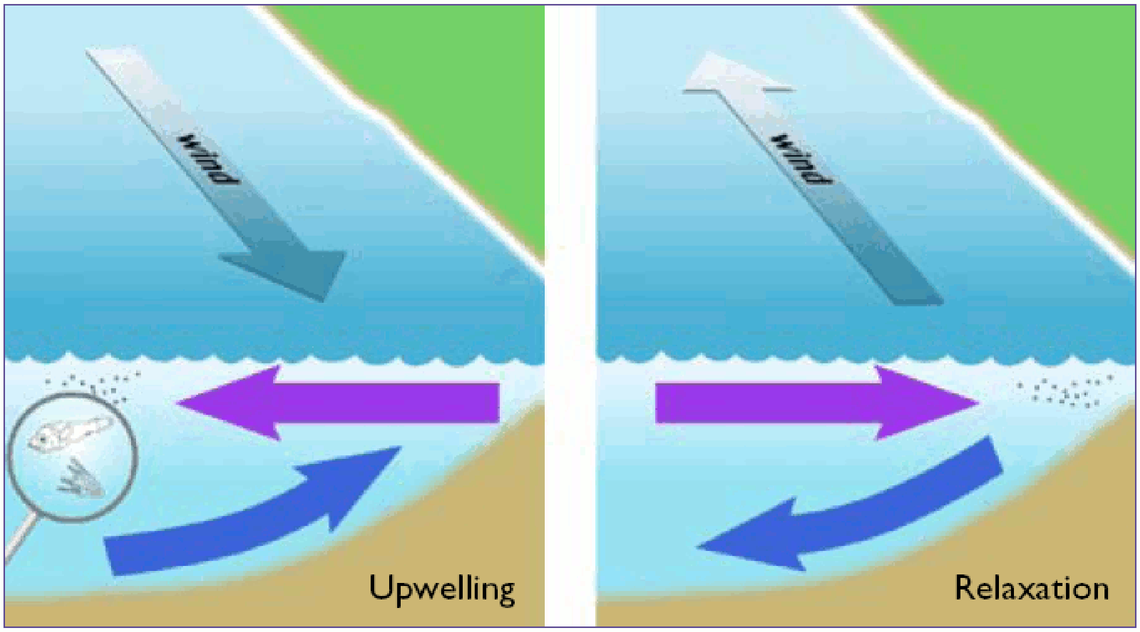

Figure 22: Upwelling off the coast of Oregon. Summer (left) and Winter (right).

The "Upwelling Index Anomaly" is a measure of the strength of upwelling in a given year. Figure 23 illustrates the value for this index since the late 1940's at 45N. While some data suggests an increase in upwelling over the last 50 years off the southern Oregon coast (42N) the results are inconclusive (OCAR 2010).

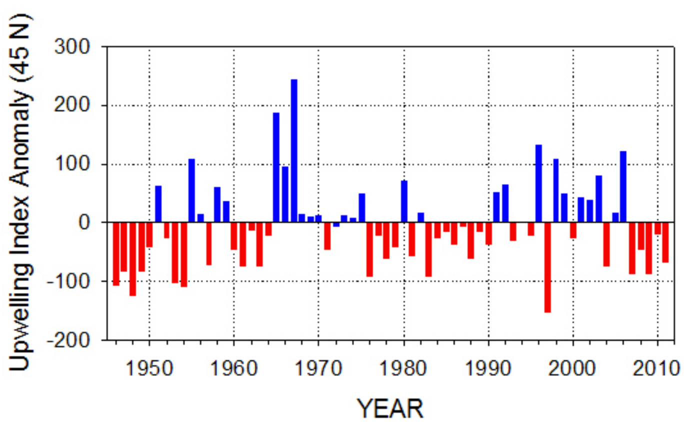

Figure 23: Upwelling Index Anomaly. Blue bars indicate stronger than average upwelling; red indicates weaker than average (www.nwfsc.noaa.gov).

Waves/Storms

The evidence for changes in wind speed and wave heights off the west coast is inconclusive, and interpretation of the data is controversial (NRC 2012). The data for wind speed and wave height analysis is typically only available for a few decades. This scarcity of data makes it difficult to distinguish any signal due to long-term climate change from that due to natural interannual-interdecadal variability (such as that associated with the PDO).

However, given the above caveat, some research does suggest long-term changes (increases) in wave height and wind speed in the northeast Pacific Ocean. Figure 24 illustrates this increase in the 99th percentile significant wave height (the average wave height of the highest one-third of all waves) and wind speed. Note that the coast of Oregon is situated in an area that shows an increase in both these quantities.

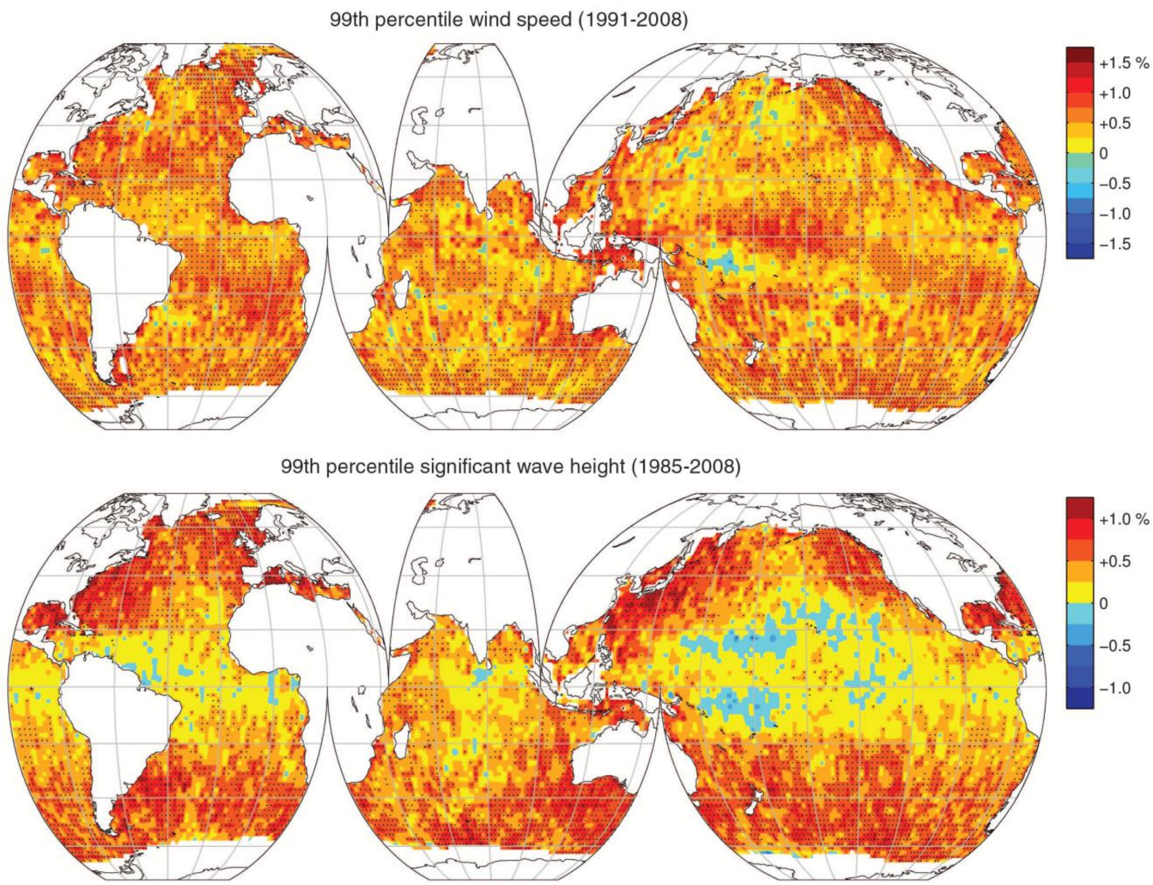

Figure 24: 99th percentile wind speed and significant wave height (Young et al. 2011).

Mean sea level rise may interact with local high water events in a synergistic way to increase the frequency of flood events. This effect is evident along the entire US coast, and is pronounced on the west coast. Even for those locations where relative sea level rise is low (such as the Oregon coast), a substantial increase in what are considered flood events may occur. For instance, by 2050 two locations on the

Oregon coast (Charleston, Coos Bay, and South Beach, Yaquina River) are projected to experience what are currently 100 year flood events every 5 years (Tebaldi et al. 2012).

Sea Surface Temperatures

Nicholls et al. (2007) observed an increase in global mean sea surface temperature (SST) of approximately 0. 6 °C/1.1 °F since 1950. This trend is projected to continue, leading to an increase in the winter average SST for most of the northern Pacific of 1.0-1.6 °C/1.8 -2.9 °F, as compared to the baseline of 1980-1999 (Overland and Wang 2007).

The SST is an important factor in a number of oceanographic and weather processes. For instance, a number of changes to marine ecosystems have been observed in response to increased air and/or sea surface temperatures. In the north Pacific, changes have been noted in algal, plankton and fish abundance (IPCC Summary for Policymakers, WG II 2007). Among these changes are the spread of warm water species due to increased temperatures (IPCC Summary for Policymakers, WG II 2007). Altered nutrient availability and primary production have also been observed as a result of increased temperatures (Hoegh-Guldberg and Bruno 2010).

As mentioned earlier, increased water temperatures have a direct impact on sea level rise. In addition, warmer SSTs contribute to increased storm intensity and greater stratification of the water column (Hoegh-Guldberg and Bruno, 2010).

Extremes

An increase in the mean value of a particular climate variable (temperature, for example) may be accompanied by an increase in the probability of extreme events as well. See figure 25. While in this example the previous climate had “Hot” days, a change (increase) in the mean essentially shifts the entire range of values higher, and therefore increases the probability of these “Hot” days (illustrated by the pink zone in the figure). In addition, an increase in the mean could allow for the occurrence of temperatures previously not experienced (red zone).

When discussing extreme events, it is important to consider what metrics are useful for answering the question(s) at hand. For instance, is the value of interest the absolute maximum seasonal temperature reached? Or, is the number of consecutive days at a slightly lower temperature more important? The Climate Index (CLIMDEX) project at www.climdex.org catalogs a variety of useful climate indices. Among the indices are metrics such as the number of frost days and the growing season length.

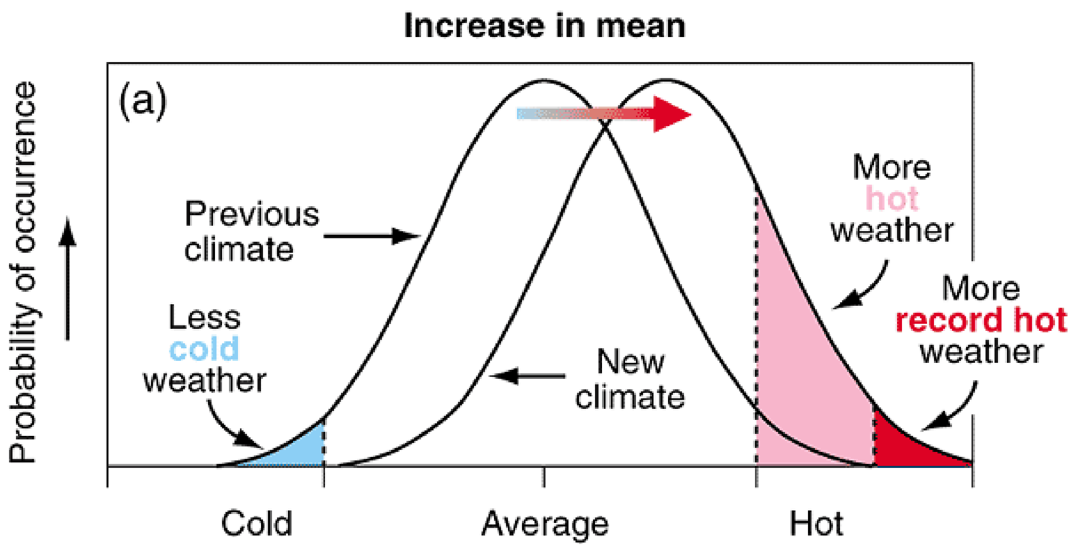

Figure 25: Increase in mean temperature (Folland et al. 2001).

Summary

Table 6 summarizes the findings of this report. As explained earlier, due to the uncertainties involved, it is not possible to give a single definitive answer as to what to expect for future climate for the lower Coquille watershed. A more defensible approach is to present the range of possible future outcomes based on ensembles of projections (when available). The temperature and precipitation projections below are based in part on original research done for this report by OCCRI, while the other results are based on a survey of the best available science. All projections are based on scenarios and conditions that might reasonably be assumed to occur in the time period specified.

Climate Parameter	**Projection(s)**
Temperature	2040s: Increase in the annual mean temperature of 1.3°C/2.3°F, range 0.7-1.9°C/1.3-3.4°F. 2060s: Increase in the annual mean temperature of 1.8°C/3.2°F, range 1.2-2.6°C/2.1-4.7°F. For both decades, the summer months have the largest projected temperature increase, as well as the largest projection range.
Precipitation	2040s and 2060s: The data suggest drier summers. Inconclusive as to whether annual precipitation will increase or decrease. Data suggests an increase in winter extreme precipitation events.
Ocean Acidification	pH will drop (i.e. increased acidification). Annual mean pH by 2050 projected to drop to 7.82 ± 0.04 (10 km nearshore, A2 emissions).
Local Relative Sea Level Rise	Somewhat less than the global average sea level rise (due primarily to local tectonics). Projections for Coos Bay, OR (in inches) = 3.5"by 2030; and 9.4" 2050.
Hydrology/ Stream Flow	High seasonality (may be enhanced). No historic trend. Possible increase in flooding events.
Upwelling	Inconclusive. Some data suggests increased upwelling.
Waves/ Storms	Suggestion of increased waves/storms. Data suggest more frequent flood events, with some west coast locations experiencing 100 year events every 5 years.
Sea Surface Temperatures	Increase on the order of 1.0°C/1.8°F (A1B) by mid-century.

Table 6: Lower Coquille watershed report summary.

Citations

Barton, A., Hales, B., Waldbusser, G. G., Langdon, C., Feely, R. A., The Pacific oyster, Crassostrea gigas, shows negative correlation to naturally elevated carbon dioxide levels: Implications for near-term ocean acidification effects, Limnology and Oceanography 57 (3), 698-710, (2012), doi:10.4319/lo.2012.57.3.0698

Bindoff, N.L., J. Willebrand, V. Artale, A, Cazenave, J. Gregory, S. Gulev, K. Hanawa, C. Le Quéré, S. Levitus, Y. Nojiri, C.K. Shum, L.D. Talley and A. Unnikrishnan, 2007: Observations: Oceanic Climate Change and Sea Level. In: Climate Change 2007: The Physical Science Basis. Contribution of Working Group I to the Fourth Assessment Report of the Intergovernmental Panel on Climate Change [Solomon, S., D. Qin, M. Manning, Z. Chen, M. Marquis, K.B. Averyt, M. Tignor and H.L. Miller (eds.)]. Cambridge University Press, Cambridge, United Kingdom and New York, NY, USA.

Coumou, D., Rahmstorf, S., A decade of weather extremes, Nature Climate Change, ,(2012), doi:10.1038/nclimate1452

Dominguez, F., Rivera, E., Lettenmaier, D. P., Castro, C. L., Changes in winter precipitation extremes for the western United States under a warmer climate as simulated by regional climate models, Geophysical Research Letters 39 (5), (2012), doi:10.1029/2011GL050762

Doney, S. C., Fabry, V. J., Feely, R. A., Ocean Acidification: The Other CO_2 Problem. Annu. Rev. Marine. Sci. 2009.1:169-192., (2009), Download at http://www.annualreviews.org/doi/pdf/10.1146/annurev.marine.010908.163834

Feely, R. A., Sabine, C. L., Byrne, R. H., Millero, F. J., Dickson, A. G., Wanninkhof, R., Murata, A., Miller, L. A., Greeley, D. Decadal changes in the aragonite and calcite saturation state of the Pacific Ocean, Global Biogeochem. Cycles, 26, GB3001, (2012), doi:10.1029/2011GB004157

Folland, C.K., Karl, T. R., Christy, J. R., Clarke, R. A., Gruza, G. V., Jouzel, J., Mann, M. E., Oerlemans, J., Salinger, M. J., Wang, S.-W., 2001: Observed Climate Variability and Change. In: Climate Change 2001: The Scientific Basis. Contribution of Working Group I to the Third Assessment Report of the Intergovernmental Panel on Climate Change Houghton, J.T.,Y. Ding, D.J. Griggs, M. Noguer, P.J. van der Linden, X. Dai, K. Maskell, and C.A. Johnson (eds.)]. Cambridge University Press, Cambridge, United Kingdom and New York, NY, USA, 881pp.

Gruber, N., Hauri, C., Lachkar, Z., Loher, D., Frolicher, T., Plattner, G-K., Rapid Progression of Ocean Acidification in the California Current System, Science 337 (6091), 220-223, (2012), doi:10.1126/science.1216773

Hansen, J., Ruedy, R., Sato, M., Lo, K., Global surface temperature change, Reviews of Geophysics 48, (2010), doi:10.1029/2010RG000345

Hawkins, E., Sutton, R., The potential to narrow uncertainty in regional climate predictions, Bulletin of the American Meteorological Society (BAMS) 90, 1095-1107, (2009), doi:10.1175/2009BAMS2607.1

Hoegh-Guldberg, O., Bruno, J. F., The impact of climate change on the world's marine ecosystems, *Science* 328, 1523-1528, (2010)

IPCC, 2007: Summary for Policymakers, WG I. In: Climate Change 2007: The Physical Science Basis. Contribution of Working Group I to the Fourth Assessment Report of the Intergovernmental Panel on Climate Change [Solomon, S., D. Qin, M. Manning, Z. Chen, M. Marquis, K.B. Averyt, M.Tignor and H.L. Miller (eds.)]. Cambridge University Press, Cambridge, United Kingdom and New York, NY, USA.

IPCC, 2007: Summary for Policymakers, WG II. In: Climate Change 2007: Impacts, Adaptation and Vulnerability. Contribution of Working Group II to the Fourth Assessment Report of the Intergovernmental Panel on Climate Change, M.L. Parry, O.F. Canziani, J.P. Palutikof, P.J. van der Linden and C.E. Hanson, Eds., Cambridge University Press, Cambridge, UK, 7-22

Komar, P. D., Allan, J. C., Ruggiero, P., Sea Level Variations along the U.S. Pacific Northwest Coast: Tectonic and Climate Controls, Journal of Coastal Research27 (5), 808-823, (2011), doi:10.2112/JCOASTRES-D-10-00116.1

Manning, M. R., Edmonds, J., Emori, S., Grubler, A., Hibbard, K., Joos, F., Kainuma, M., Keeling, R. F., Kram, T., Manning, A. C., Meinshausen, M., Moss, R., Nakicenovic, N., Riahi, K., Rose, S. K., Smith, S., Swart, R., van Vuuren, D. P., Misrepresentation of the IPCC CO2 emission scenarios, Nature Geoscience 3, 376 – 377, (2010), doi:10.1038/ngeo880

Mauger, G. S., Mantua, N., Climate Change Projections for USFS land in Oregon and Washington, University of Washington Climate Impacts Group (2011), www.cses.washington.edu/data/usfs_orwa.shtml

National Research Council (NRC) Committee on Sea Level Rise in California, Oregon, and Washington, Sea-Level Rise for the Coasts of California, Oregon, and Washington: Past, Present, and Future (2012), www.nap.edu/catalog.php?record_id=13389

Neiman, P. J., Ralph, F. M., Wick, G. A., Lundquist, J. D., Dettinger, M. D., Meteorological Characteristics and Overland Precipitation Impacts of Atmospheric Rivers Affecting the West Coast of North America Based on Eight Years of SSM/I Satellite Observations.,, **9**, 22–47, (2008), doi: http://dx.doi.org/10.1175/2007JHM855.1

Nicholls, R. J., et al. "Coastal systems and low-lying areas." Climate Change 2007: Impacts, Adaptation and Vulnerability, Contribution of Working Group II to the Fourth Assessment Report of the Intergovernmental Panel on Climate Change. Edited by M. L. Parry, O. F. Canziani, J. P. Palutikof, P. J. van der Linden and C. E. Hanson. Cambridge, UK: Cambridge University Press, (2007), 315-356

NOAA ESRL, www.esrl.noaa.gov

Ocean Carbon and Biogeochemistry Program, Subcommittee on Ocean Acidification. December 2, 2008. Ocean Acidification- Recommended Strategy for a U.S. National Research Program

Oregon Climate Assessment Report (OCAR) (2010), www.occri.net/ocar

Overland, J. E., Wang, M., Future climate of the North Pacific Ocean. Eos 88 16, 178-182, (2007)

Roe, G. H., Baker, M. B., Why Is Climate Sensitivity So Unpredictable?, Science 318, 629-632, (2007), doi:10.1126/science.1144735

Smith, E., Baker, J., Pacific Island Ecosystem Complex, from Osgood, K. E. (editor). August 2008. Climate Impacts on U.S. Living Marine Resources: National Marine Fisheries Service Concerns, Activities and Needs, U.S. Dep. Commerce, NOAA Tech. Memo. NMFS-F/SPO-89, 118 p

Tebaldi, C., Strauss, B. H., Zervas, C. E., Modeling sea level rise impacts on storm surges along US coasts, Environ. Res. Lett. 7 (2012), doi:10.1088/1748-9326/7/1/014032

USHCN, www.cdiac.ornl.gov/epubs/ndp/ushcn/ushcn.html

Vermeer, M., Rahmstorf, S., Global sea level linked to global temperature, Proceedings of the National Academy of Sciences (PNAS) 106, 21527-21532 (2009), doi:10.1073/pnas.0907765106 van Vuuren, D., Edmonds, J., Kainuma, M., Riahi, K., Thomson, A., Hibbard, K., Hurtt, G., Kram, T., Krey, V., Lamarque, J-F., Masui, T., Meinshausen, M., Nakicenovic, N., Smith, S., Rose, S.,The representative concentration pathways: an overview, Climatic Change 109, 5-31, (2011), doi:10.1007/s10584-011-0148-z

Young, I. R., Zieger, S., Babanin, A. V., Global Trends in Wind Speed and Wave Height, Science 332, 451-455, (2011), doi:10.1126/science.1197219